THREE-DIMENSIONAL DESIGN ANALYSIS FOR HYSTERETIC BEHAVIOR OF TINI-SMA FIBER EMBEDDED SMART COMPOSITES

M. Kawai

Institute of Engineering Mechanics
University of Tsukuba, Tsukuba 305-8573, JAPAN

SUMMARY: Mechanical behavior of a unidirectional TiNi shape-memory alloy (SMA) fiber embedded composite is analyzed using a three-dimensional micromechanical method of cells and a SMA model for rhombohedral and martensitic transformations. The overall behavior of the TiNi-SMA composite is governed by the pseudoelastic response of the embedded TiNi-SMA fibers, and a pseudoelasticity-like hysteretic behavior appears in the stress-strain relationships under isothermal loading and unloading conditions. The shape and size of the hysteresis are significantly influenced by the volume fraction of TiNi-SMA fibers. For a high volume fraction of fibers, in particular, the rhombohedral transformation of the embedded TiNi-SMA characterizes the overall hysteretic behavior of the TiNi-SMA composite.

KEYWORDS: Shape Memory Alloy Composite, Smart Composite, TiNi-SMA Fiber, Method of Cells, Multiaxial Constitutive Model, Pseudoelasticity, Martensitic Transformation, Rhombohedral Transformation

INTRODUCTION

For optimum designs of SMA composite systems and structures, it is necessary to evaluate the fabrication condition under which the properties of SMAs are effectively reflected and the thermomechanical condition under which they appropriately work as intended. For example, an effective combination of SMA and matrix materials and suitable shapes and a volume-fraction of SMA embedded into parent phase have to be determined. For these purposes, it would be rational if a method based on numerical simulations could be used. In this respect, it is very important to establish reliable constitutive models for predicting the thermoelastic behavior of SMA composites. When SMA composites are subjected to arbitrary thermomechanical loads, the local states of stress and strain of the SMA embedded into matrix materials always become multiaxial, and they have a significant influence on the local state of phase transformation. For accurately evaluating the performance characteristics of SMA composites, therefore, two requirements should be fulfilled. The first requirement is to furnish the SMA constitutive models which can precisely describe the phase transformation of SMAs under arbitrary multiaxial thermomechanical loading conditions. The second is to establish a homogenization method which provides an efficient procedure for a prediction of

the overall composite behavior reflecting the transformation of embedded SMAs.

The objective of the present study is to examine the mechanical behavior of TiNi-SMA fiber embedded unidirectional composites through micromechanical analyses. It is emphasized to elucidate how the pseudoelastic response of the embedded TiNi-SMA fibers under the tensile loading conditions influences on the overall behavior of unidirectional TiNi-SMA composites. For this subject, a modified multiaxial constitutive model which can describe the stress-induced rhombohedral and martensitic transformations of TiNi-SMAs under multiaxial stress conditions is developed on the basis of the phenomenological SMA constitutive models [1, 2]. By combining this TiNi-SMA model with the method of cells [3], a three-dimensional micromechanical model to predict the average behavior of unidirectional TiNi-SMA composites is constructed. Numerical simulations are carried out to observe the stress-strain relationships of unidirectional TiNi-SMA/Epoxy laminae under isothermal off-axis tensile loading and unloading conditions for different volume fractions of fibers.

MULTIAXIAL DESCRIPTION OF R-PHASE AND M-PHASE TRANSFORMATIONS FOR TINI-SMA AND APPLICATION TO COMPOSITE ANALYSIS

Constitutive Equations for Multiaxial Phase-Transformation Behavior

The pseudoelastic and shape-memory behavior of TiNi-SMAs take place due to the rhombohedral (R-phase) transformation as well as the martensitic (M-phase) one. Since the pseudoelasticity and shape-memory effect caused by the R-phase transformation have higher repeatability, much attention is paid to applications of this mechanism in practical points of view. For this reason, a phenomenological multiaxial constitutive model to describe the R- and M-phase transformations of isotropic TiNi-SMAs is developed on the basis of the uniaxial Tanaka model [1] and multiaxial Boyd-Lagoudas model [2].

The rate of the deviatoric transformation strain $\varepsilon_{ij}^{tr(x\to y)}$ during the transformation from x-phase to y-phase is expressed as

$$\dot{\varepsilon}_{ij}^{tr(x\to y)} = \Lambda_{ij}^{x\to y}\dot{z} \tag{1}$$

where z represents the volume fraction of the y-phase. The transformation tensor $\Lambda_{ij}^{x\to y}$ is given by

$$\Lambda_{ij}^{x\to y} = H^{*(x\to y)}\begin{cases} N_{ij}^{\sigma}, & \dot{z} > 0 \\ N_{ij}^{\varepsilon}, & \dot{z} < 0 \end{cases} \tag{2}$$

$$N_{ij}^{\sigma} = \frac{3}{2}\frac{s_{ij}}{\sigma_e} \tag{3}$$

$$N_{ij}^{\varepsilon} = \frac{\varepsilon_{ij}^{tr}}{\varepsilon_e^{tr}} \tag{4}$$

where s_{ij}'s are the deviatoric stress tensor, and σ_e, ε_e^{tr} denote the equivalent stress and the equivalent transformation strain of von Mises type, respectively. The superscripts (x, y)

represent the pairs of (A, R), (R, M) or (A, M): *A*, austenitic phase; *R*, rhombohedral phase; *M*, martensitic phase. The volume fraction z is expressed as $z = \eta$ and $z = \xi$ for the R-phase and M-phase transformations, respectively. Note that in this article the index e is used in two different ways; the subscript e is employed to represent the equivalent scalar quantities of von Mises type, and the superscript e to denote the elastic strain tensor.

The coefficient $H^{*(x\to y)}$ prescribes the range of the transformation strain which appears while the volume fraction z changes from 0 to 1. In this study, the expression of $H^{*(x\to y)}$ was assumed as

$$H^{*(x\to y)} = -\frac{\Gamma^{*(x\to y)}}{E^{x\to y}(z)} + \frac{E^y - E^x}{[E^{x\to y}(z)]^2}\sigma_e - (\alpha^y - \alpha^x)\Delta T \tag{5}$$

where $\Gamma^{*(x\to y)} = \Psi^*$ when $z = \eta$, and $\Gamma^{*(x\to y)} = \Omega^*$ when $z = \xi$. The temperature difference ΔT is taken from a stress free reference temperature T_0, i.e. $\Delta T = T - T_0$. The change in the Young's modulus $E^{x\to y}(z)$ during the phase transformation is described as

$$E^{x\to y}(z) = E^x + z(E^y - E^x) \tag{6}$$

Kinetics of Phase Transformation

The evolution equations of the phase volume fractions (η and ξ) for TiNi-SMAs under uniaxial tensile loading conditions were identified by Lin et al. [4]. In the present study, a simple extension to a multiaxial form compatible with the SMA model described above has been assumed as follows:

Replacing the uniaxial stress with the von Mises equivalent stress, we can obtain the following multiaxial expression in a compact form:

$$\dot{z} = (-1)^{\lambda^{x\to y}} z^{m^{x\to y}} (1-z)^{n^{x\to y}} b^{x\to y}\left(c^{x\to y}\dot{T} - \dot{\sigma}_e\right) \tag{7}$$

where the coefficients involved by this equation take different values for the forward and reverse transformations of R-phase and M-phase.

From these evolution equations for the volume fractions of R-phase and M-phase, we can determine the transformation start and finish stresses:

$$\sigma_e^Y = d^{x\to y}(T - T^{x\to y}) - \sigma_e^{(0)} \tag{8}$$

where the superscript Y represents start or finish.

Homogenization Based on The Method of Cells

To predict the overall behavior of unidirectional SMA-fiber composites, the generalized method of cells [3] was used. In this three-dimensional micromechanics, the periodic

microstructure of continuous fiber composites is represented by a rectangular-shaped unit cell which consists of rectangular-shaped subcells; typically, one subcell corresponds to the fibers and the others to the matrix materials.

Assuming the four-subcells model of the first order, the displacement (or velocity) fields in the subcells are described as

$$v_i^{(\beta\gamma)} = w_i^{(\beta\gamma)} + \bar{x}_2^{(\beta)}\dot{\phi}_i^{(\beta\gamma)} + \bar{x}_3^{(\gamma)}\dot{\psi}_i^{(\beta\gamma)} \tag{9}$$

where $w_i^{(\beta\gamma)}$'s represent the displacements (or velocities) at the center of mass for each subcell. The last two terms in the right-hand side give variations which are linear to the local coordinate $(\bar{x}_2^{(\beta)}, \bar{x}_3^{(\gamma)})$ with respect to the origin at subcell center. The subcells are identified with pairs of Greek superscripts: (β, γ), $1 \_ \beta, \gamma \_ 2$. Summation convention is not applied to Greek indices.

Effects of damage at the interfaces of subcells can be incorporated into the method of cells by assuming the spring-like weakened interfaces. In this formulation, the displacement jumps take place only in the normal and tangential directions of the interfaces for the fiber subcell. The displacement-continuity at the subcell interfaces is partly relaxed and prescribed by the following equations:

$$w_i^{(11)} = w_i^{(12)} = w_i^{(21)} = w_i^{(22)} \equiv w_i \tag{10}$$

$$h_1\dot{\phi}_i^{(1\gamma)} + h_2\dot{\phi}_i^{(2\gamma)} + 2\lambda_1 R_{2j}^{(\gamma)}\sigma_{2j}^{(1\gamma)} = h\frac{\partial w_i}{\partial x_2} \tag{11}$$

$$\lambda_1\dot{\psi}_i^{(\beta 1)} + \lambda_2\dot{\psi}_i^{(\beta 2)} + 2h_1 R_{3j}^{(\beta)}\sigma_{3j}^{(\beta 1)} = \lambda\frac{\partial w_i}{\partial x_3} \tag{12}$$

where the coefficients $R_{2j}^{(\gamma)}$ and $R_{3j}^{(\beta)}$ represent the extent of discontinuity at the fiber-matrix interfaces, and $h = (h_1 + h_2)$ and $l = (l_1 + l_2)$.

MATERIAL IDENTIFICATION

The material constants to characterize the kinetics of the R-phase and M-phase transformations of TiNi-SMAs were determined by Lin et al. [4]. These values were assumed in the present study.

Regarding the transformation parameter $\Gamma^{*(x\to y)}$, the temperature dependence was only taken into account through

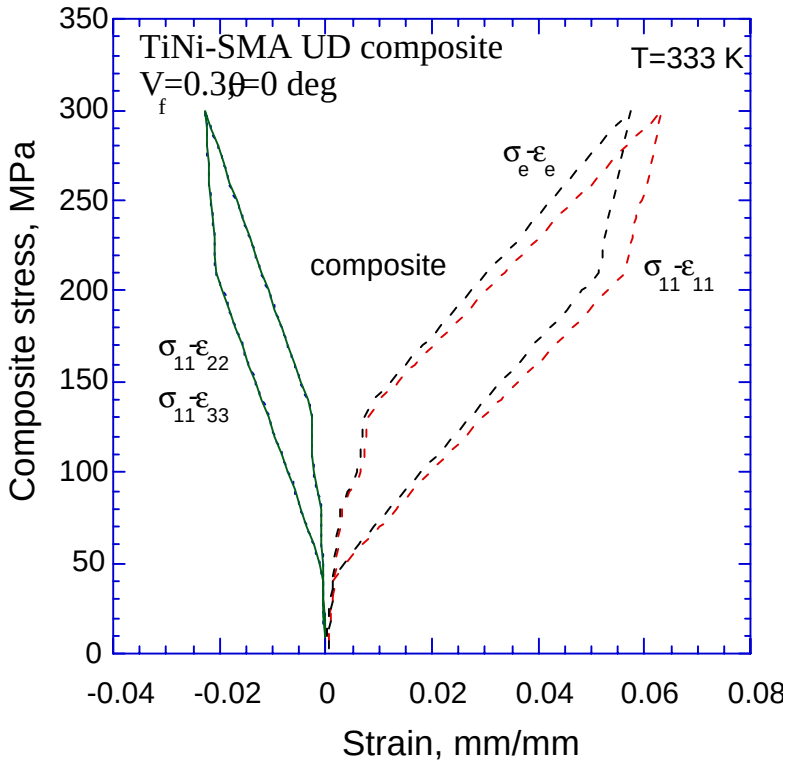

Fig. 1: Predicted behavior of TiNi-SMA composite under a longitudinal loading-unloading cycle ($\theta = 0°$, $V_f = 0.3$, $T = 333$ K)

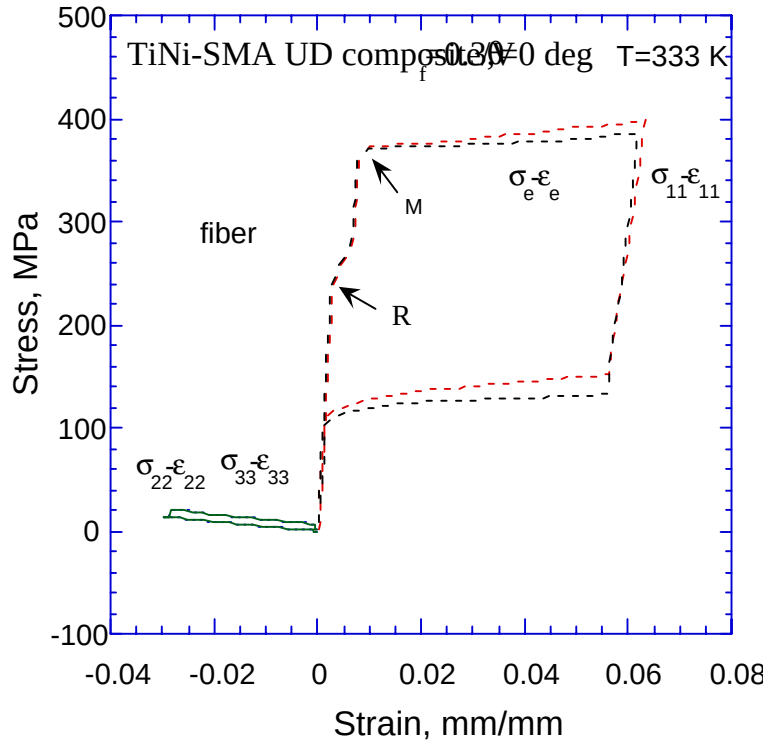

Fig. 2: Predicted behavior of embedded TiNi-SMA fibers under a longitudinal loading-unloading cycle ($\theta = 0°$, $V_f = 0.3$, $T = 333$ K)

$$\Gamma^{*(x\to y)} = \begin{cases} \Psi^* = 6.49T - 2286, & z = \eta \\ \Omega^* = -6T - 700 \quad , & z = \xi \end{cases} \tag{13}$$

These relationships were determined so as to describe the uniaxial stress-strain behavior of TiNi-SMAs observed by Lin et al. [4].

The standard epoxy resin system was chosen as a matrix material, and an isotropic and linear elastic behavior was assumed. The Young's modulus and the Poisson's ratio were specified as $E = 4.14$ GPa and $\nu = 0.3$, respectively.

RESULTS OF NUMERICAL SIMULATIONS

A single tensile loading and unloading cycle was given to the unidirectional TiNi-SMA fiber embedded epoxy composite, respectively, in the longitudinal ($\theta = 0°$), transverse ($\theta = 90°$) and off-axis ($\theta = 30°$) directions. The external stress was applied to the SMA composite up to 300 MPa in stress control. The temperature was specified to be a constant value of 333 K.

The predicted stress-strain responses of TiNi-fiber/Epoxy composite and embedded TiNi-SMA fibers [(β, γ) = (1, 1)] are shown in Figs. 1 and 2, respectively, for the longitudinal loading-unloading cycle ($\theta = 0°$, $V_f = 0.3$, $T = 333$ K, $\sigma_{max} = 300$ MPa). Note that the stress and strain components are taken with respect to the fiber coordinate system. Relations between the equivalent stress and strain (σ_e - ε_e) are also entered.

Regarding the longitudinal loading response (σ_{11} - ε_{11}) of the embedded TiNi-SMA fibers shown in Fig. 2, we can observe that the first corner appears at about 240 MPa after the linear elastic response. This corresponds to the beginning of the R-phase transformation of TiNi-SMA fibers. By increasing a small amount of stress, the parent (austenite) phase completely changes to the R-phase at 280 MPa (the second corner). After the linear increase of stress due to the elastic behavior of the R-phase, the third corner appears at about 360 MPa. This is the starting point of the M-phase transformation, and a large amount of transformation strain develops with a small increase of stress. During the subsequent unloading process, the stress-strain relationship is almost linear before the rapid recovery of the total strain begins. The corner representing the start of the reverse transformation of the R-phase to the austenite is not clearly observed. This indicates that the forward transformation from the R-phase to the M-phase is almost completely finished during the prior loading period. If the remaining R-phase is relatively large just before the unloading occurs, we will observe the corner representing the start of the reverse transformation of the remaining R-phase during unloading period. Therefore, it is found that the linear unloading curve from 400 MPa to 150 MPa represents the elastic response of the M-phase, and the succeeding rapid strain recovery with a small decrease in stress is caused by the reverse transformation of the M-phase to the austenite.

The SMA composite exhibits a large hysteresis loop for the given loading-unloading cycle, as observed in Fig. 1. Therefore, the overall loading-unloading hysteretic behavior of the SMA composite clearly reflects the pseudoelastic behavior of the embedded SMA fibers. It is

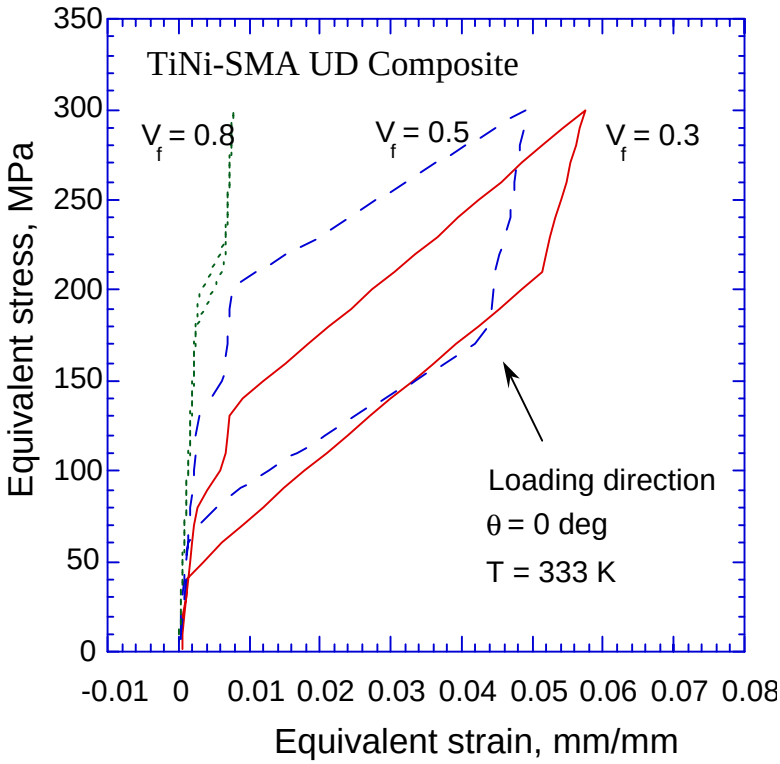

Fig. 3: Comparison between equivalent stress and strain curves for TiNi-SMA composite ($\theta = 0°$, $T = 333$ K)

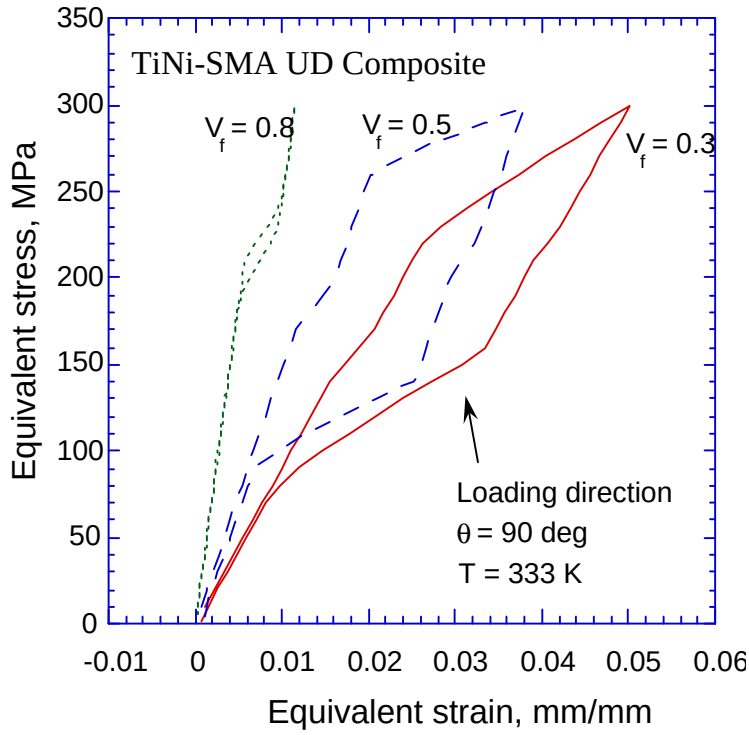

Fig. 4: Comparison between equivalent stress and strain curves for TiNi-SMA composite ($\theta = 90°$, $T = 333$ K)

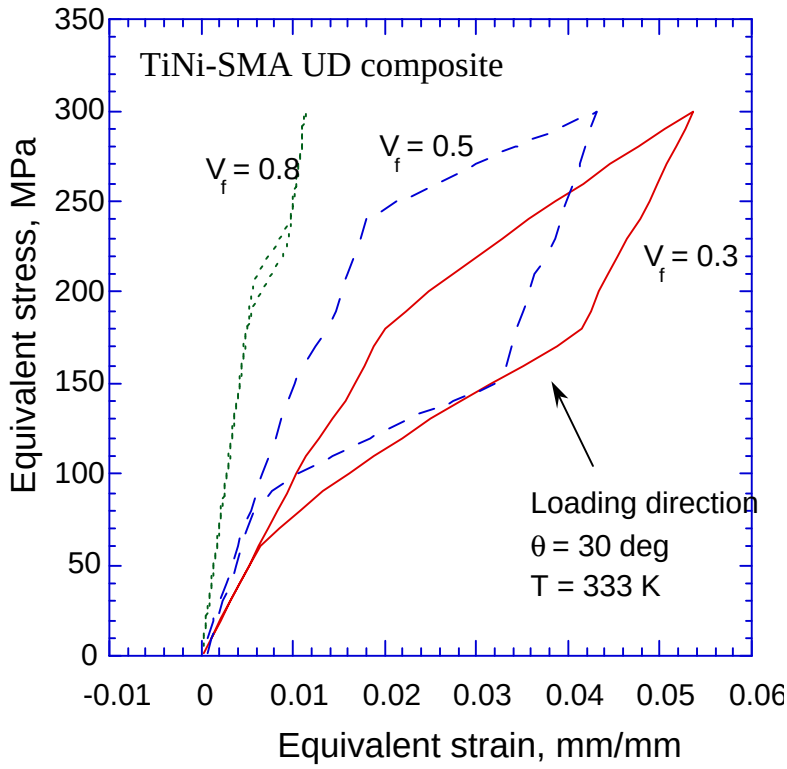

Fig. 5: Comparison between equivalent stress and strain curves for TiNi-SMA composite ($\theta = 30°$, $T = 333$ K)

noted that the shapes of the stress-strain hysteresis are different between the composite and the SMA fibers.

The equivalent stress-strain relationships of TiNi-SMA composites with different fiber volume fractions are plotted in Figs. 3, 4, and 5 for longitudinal, transverse and off-axis loading conditions, respectively, to compare the influences of the fiber volume fraction and the loading direction on the overall composite behavior.

From these simulations, we can obtain two important results. The first one is that the overall behavior is clearly influenced by the phase transformation behavior of the embedded SMA fibers. The extent of this influence significantly depends on the fiber volume fraction. It is important to note that the hysteretic behavior of the SMA composite does not completely coincide with the pseudoelastic response of the embedded SMA fibers. Therefore, the composite analyses as presented in this study become very important to evaluate the characteristics of the SMA composite and the performance of SMA-based smart structures. In the second, it is clearly indicated that an appropriate formulation of the multiaxial constitutive model for describing the transformation behavior of SMAs is of great significance for the analysis-based designs of SMA composite smart structures. If the constitutive model assumed could not describe the R-phase transformation of TiNi-SMA fibers, the hysteretic behavior of the composite for $V_f = 0.8$ shown in Figs. 3 through 5 would not have been predicted; instead, just linear elastic responses would have been obtained.

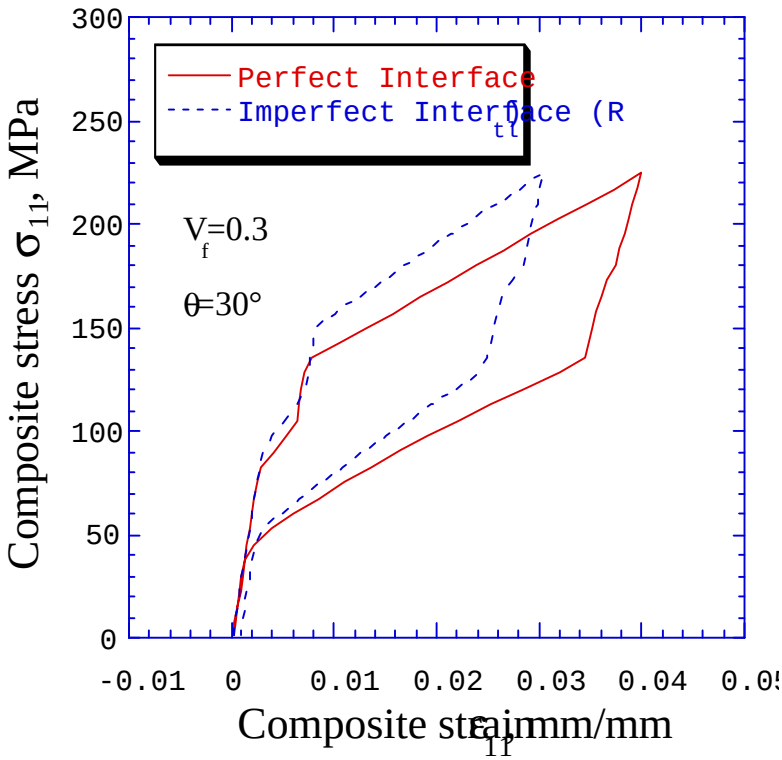

Fig. 6: Stress-strain curves for TiNi-SMA/Epoxy lamina with perfect and imperfect interfaces under off-axis tensile loading

An effect of imperfect bonding at the interfaces between SMA fibers and matrix on the overall behavior of SMA composite is demonstrated in Fig. 6 for the case that the response of the epoxy resin is linearly elastic.

CONCLUSION

A simple procedure to evaluate the characteristics of the TiNi-SMA composites was developed by combining the three-dimensional method of cells with the multiaxial constitutive model which was able to describe the stress-induced rhombohedral and martensitic transformations of TiNi-SMAs. The mechanical behavior of the unidirectional TiNi-SMA/Epoxy composites subjected to a single isothermal loading and unloading cycle was analyzed for different fiber volume fractions and loading directions. Based on these numerical calculations, effects of the pseudoelastic response of TiNi-SMA fibers embedded into an epoxy matrix on the overall behavior of the SMA composite were examined.

It was thus demonstrated that the multiaxial SMA constitutive model developed to describe both R-phase and M-phase transformations of TiNi-SMAs and its combination with the method of cells provided efficient tools for analysis-based designs of SMA composites and structures.

REFERENCES

1. Tanaka, K. «A Phenomenological Description on Thermomechanical Behavior of Shape Memory Alloys», *Elastic-Plastic Failure Modelling of Structures With Applications*, HUI, D. and KOZIK, T.J. Ed., PVP-Vol. 141, 1988, pp. 163-170.

2. Boyd, J. G. and Lagoudas, D.C., «Thermomechanical Response of Shape Memory Composites», *Journal of Intelligent Material Systems and Structures*, Vol. 5, 1994, pp. 333-346.

3. Paley, M. and Aboudi, J.A., «Micromechanical Analysis of Composites by the Generalized Cells Model», *Mechanics of Materials*, Vol. 14, 1992, pp. 127-139.

4. Lin, P., Tobushi, H., Tanaka, K., Hattori, T. and Uchino, K., «Deformation Properties Associated with Martensitic and R-phase Transformation in TiNi Shape Memory Alloy», *Transaction of JSME*, Vol. 60A, No. 569, 1994, pp 126-133.